



Research Article

Biosorption of Ni²⁺ and Cr³⁺ in synthetic sewage: Adsorption capacities of water hyacinth (*Eichhornia crassipes*)

Francis James OGBOZIGE^{*1}, Helen Uzoamaka NWOBUN²

¹Department of Civil Engineering, Federal University Otuoke, Nigeria

²Department of Chemical Engineering, University of Lagos, Nigeria

ARTICLE INFO

Article history

Received: 09 August 2021

Revised: 24 October 2021

Accepted: 01 November 2021

Key words:

Freundlich; Halsey; Harkin-Jura;
Langmuir; Temkin

ABSTRACT

Water hyacinth (*Eichhornia crassipes*) is an aquatic weed that is causing numerous adverse effects on freshwater bodies. Developing countries are still battling on how to control the growth of this weed without damaging other aquatic lives important to man. Literatures have revealed that most developing countries are still discharging untreated sewage containing heavy metals into waterbodies due to economic and technical constraints in handling conventional methods of treating heavy metals. Hence, the research investigated the possibility of using water hyacinth to adsorb heavy metals (Ni²⁺ and Cr³⁺) from sewage before discharging into waterbodies in order to solve two major problems faced in the aquatic environment, at minimal cost. This was achieved by using the said weed (water hyacinth) to treat Ni²⁺ and Cr³⁺ solutions prepared in the lab. Results showed that the adsorption process for both ions occurred on heterogeneous surfaces while the mechanism of adsorption followed Pseudo 2nd-order kinetics. The Freundlich, Langmuir and Temkin adsorption capacities for Ni²⁺ are 19.6925l/g, 0.7470l/mg and 1.1093l/mg respectively while for Cr³⁺ are 16.814l/g, 0.7011l/mg and 0.9623l/mg respectively. However, the heat of sorption for Ni²⁺ is 96.906KJ/mol while that of Cr³⁺ is 98.749KJ/mol. Furthermore, FT-IR analysis identified seven functional groups involved in the binding sites with more of hydroxyl group (O-H) from alcohol and carboxylic acid. It was concluded that water hyacinth could be used as a potential bio-adsorbent of metal ions.

Cite this article as: Ogbozige FJ, Nwobun HU. Biosorption of Ni²⁺ and Cr³⁺ in synthetic sewage: Adsorption capacities of water hyacinth (*Eichhornia crassipes*). Environ Res Tec 2021;4:4:342–351.

INTRODUCTION

Several researchers including Obasi and Akudinobi [1–3] have reported alarming concentrations of heavy metals in institutional and industrial effluents especially in developing countries even after been treated. This is because the sewage are mostly treated in either waste stabilization pond (WSP), tricking filter (TF) or activated sludge pro-

cess (ASP) without further treatment. Hence, the wastewaters are merely treated in terms of reducing the biochemical oxygen demand (BOD) or chemical oxygen demand (COD) and bacteriological load to permissible limits since the technology associated with WSP, TF and ASP cannot treat or reduce heavy metals. Thus, the discharge of such effluents into water bodies is still dangerous even if the concentrations of BOD, COD and bacteriological load are safe.

*Corresponding author.

*E-mail address: engr.ogbozige@gmail.com



Consumption of food items containing heavy metals has long been identified to have numerous effects on human health [4–6]. Heavy metals bio-accumulate in both plants and animals [7] hence if discharged into streams and rivers, it could be incorporated into planktons and fishes which will consequently affect humans through the food chain.

The standard methods for reducing the concentrations of heavy metals in sewage to permissible levels, which includes membrane filtration, chemical precipitation and ion exchange have been identified to have technical and economic setbacks when applied in developing countries. Past literatures [8–10] have shown that bioadsorbents could be effectively used in removing heavy metals in wastewaters. However, the availability of most of these bioadsorbents such as coconut shell, orange peels, groundnut shell, cassava peels as well as banana and plantain peels are low compared to the volume of industrial and institutional sewage generated daily. Water Hyacinth (*Eichhornia crassipes*) is an aquatic weed that is readily available in polluted freshwater bodies. It grows very fast hence, it hampers the movement of boats and canoes in rivers during navigation as could be seen in Figure 1. It also deteriorates the turbidity and dissolved oxygen content of the affected river, causing negative impacts on the production of phytoplankton and fishes and even affecting the use of the river for recreational and fishing activities. It makes riparian communities to be prone to flooding during rainy season since the rate of outflow to draining water bodies is low due to the resistance to free flow caused by it. In other words, the infestation of water hyacinth (*Eichhornia crassipes*) in a water body has both ecological and socio-economical effects on the affected communities.

Nickel (Ni) and chromium (Cr) are among the common heavy metals usually found in industrial and institutional sewage [11]. Yet, researchers on heavy metals adsorption rarely worked on these two metals. In addition, despite the abundance availability of this aquatic weed (*Eichhornia crassipes*), literatures on the subject matter is still scarce. Hence, it is important to investigate its usefulness in adsorbing nickel and chromium ions (Ni^{2+} , Cr^{3+}) which have been reported to be among the common heavy metals in industrial and institutional sewage. This will serve as a means of removing both the aquatic weed from the affected rivers as well as the heavy metals from industrial sewage, together with their associated adverse effects.

MATERIALS AND METHODS

Preparation of Adsorbent and Synthetic Sewage

Fresh water hyacinths (*Eichhornia crassipes*) were obtained at the Oxbow Lake in Yenagoa, Nigeria (4°54'26.83"N, 6°16'43.29"E) and were carefully washed with tap water to remove the sand and silt particles attached in the roots. Thereafter, distilled water was used in rinsing the washed water hyacinth, sun dried for 48 hours and further dried



Figure 1. Impact of water hyacinth in river transportation.

in an oven (model E028–230V-T) at 105°C for 12 hours. The dried water hyacinths were milled using a laboratory-grinding machine (EcoMet 30) and the particles were sieved through a 250µm mesh. Since, the weed (water hyacinth) is abundantly available, it was not modified with any reagent hence, the 250µm sieved particles were kept in an airtight polyethylene container as the bioadsorbent to be used for the adsorption process.

Industrial sewage containing Ni^{2+} and Cr^{3+} (i.e. adsorbate) were synthesized in the laboratory by preparing a stock solution of 1000 ppm (i.e. 1000 mg/l) for each using the analytical grades of their hydrated nitrates salts $\text{Ni}(\text{NO}_3)_2 \cdot 6\text{H}_2\text{O}$ and $\text{Cr}(\text{NO}_3)_3 \cdot 9\text{H}_2\text{O}$ respectively. However, the quantity of the various salts used in preparing the stock solutions of 1000ppm were determined through Equation (1);

$$M = \frac{M_m}{A_m} \times \frac{V}{1000} \times \frac{100}{P_p} \quad (1)$$

In Equation (1), M is the mass of salt weighed in gram (g), M_m is the molecular mass of the salt, A_m is the atomic mass of the metal considered, V is the volume of distilled water used in dissolving the salt in milliliter (ml) and P_p is the percentage of purity of the salt.

The level of purity for both $\text{Ni}(\text{NO}_3)_2 \cdot 6\text{H}_2\text{O}$ and $\text{Cr}(\text{NO}_3)_3 \cdot 9\text{H}_2\text{O}$ is 99.99% and were supplied by Alfa Aesar company, Ward Hill, Massachusetts, USA while the volume prepared for each stock solution is 1000 ml. Also, the molecular masses of $\text{Ni}(\text{NO}_3)_2 \cdot 6\text{H}_2\text{O}$ and $\text{Cr}(\text{NO}_3)_3 \cdot 9\text{H}_2\text{O}$ are known to be 290.80 and 400.15 respectively while the atomic masses of Ni and Cr are 58.6934 and 51.9961 respectively. Hence, these information were substituted into Equation (1) to obtain 4.955g of $\text{Ni}(\text{NO}_3)_2 \cdot 6\text{H}_2\text{O}$ and 7.697g of $\text{Cr}(\text{NO}_3)_3 \cdot 9\text{H}_2\text{O}$ as the required quantity of the salts needed to produce 1000 ppm stock solutions of Ni^{2+} and Cr^{3+} respectively, using 1000 ml distilled water as solvent. However, the initial concentrations of Ni^{2+} and Cr^{3+} needed as working solutions were attained by means of serial dilution of the prepared stock solutions.

Metal Adsorption Studies

Batch adsorption was conducted to understand the impacts of certain parameters on the removal of the metal ions (Ni^{2+} and Cr^{3+}) using water hyacinth as adsorbent. The parameters considered in this research are contact time, adsorbent dosage, initial adsorbate concentration and solution pH. While studying the impact of each of the aforementioned parameters, the parameter concerned was varied while others were kept constant.

Effect of Contact Time

The effect of contact time on the adsorption process was studied by considering different contact times ranging from 10 to 100 minutes at room temperature (20–25°C). In each of the adsorbates considered (Ni^{2+} and Cr^{3+}), 25 ml having initial concentration of 2.5 mg/l and pH 7 was measured into a 50 ml beaker and a weighing machine (model: FA 1604) was used to measure 0.5 g of the water hyacinth adsorbent into the beaker. The mixture in the beakers were properly mixed by stirring at 150 rpm for different contact times (10, 20, 30,....., 100 minutes) using a magnetic stirrer (model: SH-2). The stirred mixture was filtered through a Whatman filter paper (Grade 1) and the concentration of the metal ion (Ni^{2+} or Cr^{3+}) in the filtrate was determined using atomic absorption spectrometer, AAS (model: 280FS AA). However, each of the contact time considered was studied trice and the mean value of the concentrations of metal ion obtained from the AAS was recorded.

Effect of Adsorbent Dosage

Different masses of the water hyacinth adsorbent ranging from 0.2 to 1.0 g were weighed and added separately into 50 ml beakers already containing 25 ml of 2.5 mg/l of each of the adsorbates (Ni^{2+} and Cr^{3+}) at pH 7. The mixture in the beakers were stirred at 150 rpm for a constant contact time of 50 minutes under room temperature (20–25°C), and filtered through grade 1 of Whatman filter paper. The process was repeated trice in each of the dose considered (0.2, 0.4, 0.6, 0.8, 1.0 g) and their mean concentrations of Ni^{2+} or Cr^{3+} in their respective filtrates obtained from the AAS were recorded.

Effect of Initial Adsorbate Concentration

Working solutions of Ni^{2+} and Cr^{3+} containing initial concentrations ranging from 1.0 to 5.0 mg/l at pH 7 were prepared from their respective stock solutions. This was followed by measuring 25ml of each initial concentration prepared (1.0, 2.0, 3.0, 4.0, 5.0 mg/l) for Ni^{2+} and Cr^{3+} separately into 50ml beaker, and 0.5g of the adsorbent were measured into the beakers. The mixture in the beakers were thoroughly mixed at 150 rpm for 50 minutes contact time under room temperature (20–25°C), filtered on Whatman filter paper (grade 1) and the filtrates were analysed on AAS for the concentrations of Ni^{2+} and Cr^{3+} . The procedure was replicated trice for each initial adsorbate

concentration and the average value of the metal ion gotten from the AAS was recorded.

Effect of Solution pH

The impact of this parameter (solution pH) on the removal of the metal ions was known by measuring 25 ml of 2.5 mg/l of the adsorbates (Ni^{2+} and Cr^{3+}) of different pH values ranging from 5 to 9 into 50 ml beakers separately. The varied solution pH 5, 6, 7,8, 9 were achieved by adding some drops of either 0.1M of HCl or 0.1M of NaOH into the working solutions until the desired pH value is indicated in a pH meter (model: pH-20W). Similarly, 0.5g of the water hyacinth adsorbent was added into each of the beakers containing the varied pH solutions and were properly stirred at 150 rpm for 50 minutes under room temperature (20–25°C). Thereafter, the stirred contents in the beakers were filtered through a Whatman filter paper of grade 1 and the filtrates were analysed in an AAS for the concentrations of Ni^{2+} or Cr^{3+} as the case may be. Just like the case in the other parameters earlier explained, the process was repeated trice for each of the pH solution and the mean value of the concentrations of Ni^{2+} or Cr^{3+} was recorded.

Trend Analysis of Varied Adsorption Parameters

In order to understand the impacts of the varied parameters on the adsorption process, the percentage of metal ions adsorbed for each of the varied parameters studied were determined by employing Equation (2);

$$\% \text{ adsorbed} = \left(\frac{C_0 - C_f}{C_0} \right) \times 100 \quad (2)$$

Where C_0 is the initial concentration in mg/l while C_f is the final concentration of metal ion obtained from the AAS. In each of the parameters studied (i.e. contact time, adsorbent dosage, initial adsorbate concentration and solution pH), the percentages of metal ion adsorbed for both Ni^{2+} and Cr^{3+} were plotted against their corresponding variations on 2-line graphs (one line for each metal ion). Different colour legends were assigned to the metal ions in the 2-line graphs, which help in revealing the metal ion that was adsorbed more in each variations of a given parameter.

Adsorption Isotherm Studies

The adsorption isotherm models considered in this research are Freundlich, Langmuir, Temkin, Harkin-Jura, and Halsey. Prior to their applications, the equilibrium concentrations (C_e) of the metal ions were determined by recording the concentration that remained constant even when contact times were increased. Hence, the equilibrium adsorption for each metal ion was calculated using Equation (3);

$$q_e = \frac{V(C_0 - C_e)}{M} \quad (3)$$

Where q_e is the amount of metal ion (adsorbate) adsorbed at equilibrium in mg/g, V is the volume of solution (adsor-

bate) in liters, C_0 and, C_e are the initial and equilibrium concentrations of metal ion in mg/l respectively and M is the mass of the adsorbent used in gram (g).

Among the various isotherm models studied, the model that best governs the adsorption process for each adsorbate was known by plotting the following graphs; $\log q_e$ versus $\log C_e$ (for Freundlich model), $\frac{1}{q_e}$ versus $\frac{1}{C_e}$ (for Langmuir model), q_e versus $\ln C_e$ (for Temkin model), $\frac{1}{q_e^2}$ versus $\log C_e$ (for Harkin-Jura model) and $\ln q_e$ versus $\ln C_e$ (for Halsey model). The regression equations associated with the various graphs plotted were compared with their corresponding standard isotherm models thereafter, their constants including adsorption capacities were determined from the gradients and intercepts. The isotherm model whose graph has the highest value of determination coefficient (R^2) was considered as the isotherm model governing the adsorption process. The linear form of Freundlich, Langmuir, Temkin, Harkin-Jura, and Halsey isotherm models are given in Equation 4, 5, 6, 7 and 8 respectively.

$$\log q_e = \frac{1}{n} \log C_e + \log K_f \quad (4)$$

In Equation (4), q_e is the amount of metal ion (adsorbate) adsorbed at equilibrium in mg/g, n is Freundlich constant which indicate adsorption intensity (dimensionless), C_e is the concentration of metal ion at equilibrium in mg/l and K_f is Freundlich constant which shows adsorption capacity in l/g.

$$\frac{1}{q_e} = \left(\frac{1}{K_L \cdot q_m} \right) \frac{1}{C_e} + \frac{1}{q_m} \quad (5)$$

In Equation (5), K_L is the Langmuir equilibrium constant in l/mg, q_m is the monolayer adsorption capacity at equilibrium in mg/g while q_e and C_e have same meaning as previously explained.

$$q_e = \beta \ln C_e + \beta \ln K_T \quad (6)$$

The symbols K_T and β in Equation (6) are Temkin constants indicating isotherm equilibrium binding in l/mg and heat of sorption in KJ/mol respectively while q_e and C_e remain the same.

$$\frac{1}{q_e^2} = -\frac{1}{A} \log C_e + \frac{B}{A} \quad (7)$$

As usual, q_e and C_e in Equation (7) remain the same as adsorption at equilibrium (mg/g) and equilibrium concentration (mg/l) respectively however, A and B are Harkin-Jura dimensionless constants.

$$\ln q_e = -\frac{1}{n} \ln C_e + \frac{1}{n} \ln K_H \quad (8)$$

K_H and n in Equation (8) represent Halsey isotherm constants (dimensionless) while q_e and C_e remain the same as earlier explained.

Adsorption Kinetics Studies

The pathway and mechanism of the adsorption process for each metal ion was investigated using Pseudo first order and second order kinetic models. The amount of metal ions (Ni^{2+} or Cr^{3+}) adsorbed on the adsorbent at a given contact time t was calculated and denote as (q_t) using Equation (9).

$$q_t = \frac{V(C_0 - C_t)}{M} \quad (9)$$

Where q_t is the amount metal ion adsorbed on the adsorbent in mg/g at contact time t , V is the volume of solution (adsorbate) in liters, C_0 is the initial concentration of metal ion in mg/l, C_t is the concentration of metal ion at contact time t in mg/l while M is the mass of the adsorbent used in gram (g).

For Pseudo first order kinetic model, a graph of $\log(q_e - q_t)$ versus contact time t was plotted while $\frac{t}{q_t}$ versus t was plotted for Pseudo second order kinetic model. The rate constants for the two kinetic models were determined by comparing the linear equation of the best fitted lines associated with the plotted graphs and their corresponding kinetic model equations in linear forms. The linear forms of Pseudo first and second order kinetic models are given in Equations (10) and (11) respectively.

$$\log(q_e - q_t) = -\left(\frac{k_1}{2.303}\right)t + \log q_e \quad (10)$$

$$\frac{t}{q_t} = \left(\frac{1}{q_e}\right)t + \frac{1}{k_2 \cdot q_e^2} \quad (11)$$

Where k_1 is the Pseudo first order rate constant (min^{-1}) and k_2 is the Pseudo second order rate constant ($\text{g} \cdot \text{mg}^{-1} \cdot \text{min}^{-1}$) while other symbols retained their meaning as previously explained.

Fourier Transform Infrared Spectroscopy Analysis

The functional groups responsible for the metal ions adsorption were known by analyzing the water hyacinth adsorbent before and after adsorption using a Fourier Transform Infrared (FT-IR) Spectrometer (model: IRAfinity-1S). Potassium bromide (KBr) weighing 250 mg was measured into a mortar and it was properly pulverized with the help of a pestle until it becomes sticky to the mortar. Afterward, 2.5 mg of dried sieved water hyacinth adsorbent (before adsorption) was added into the mortar. The mixture in the mortar was grinded for 3 minutes and placed in a 7 mm die set, compressed at 2 ton in a mini-pellet press made by Specac Ltd (model: P/N GS03940) for 2 minutes to form pellet. The pellets for the water hyacinth adsorbents after the adsorption process were prepared in the same manner using 2.5 mg of dried sieved residue of filtration after adsorption. In both cases, scanning of pellets were carried out at a wavenumber range of 4000 to 400 cm^{-1} in the FT-IR spectrometer and the wavenumber peaks were compared with Table 1 to understand the functional groups present.

Table 1. Wavenumber of some common functional groups

Functional group	Wavenumber (cm ⁻¹)	Assignment (vibration and intensity)
Alkane	1350 – 1480	C–H (bending and medium)
	2840 – 3000	C–H (stretch and medium)
Alkene	675 – 1000	=C–H (bending and strong)
	1648 – 1662	C=C (stretch and medium)
	1665 – 1678	C=C (stretch and weak)
	3020 - 3100	=C–H (usually sharp)
Alkyne	2100 – 2500	C≡C (stretch and weak)
	3267 – 3333	C–H (stretch and strong; usually sharp)
Alcohol	1020 – 1150	C–O (stretch and strong)
	1330 – 1420	O–H (bending and medium)
	2700 – 3200	O–H (weak and usually broad)
	3200 – 3550	O–H (stretch and strong; <u>usually broad</u>)
	3580 – 3650	O–H (variable and usually sharp)
Carboxylic acid	1395 – 1440	O–H (bending and medium)
	1700 – 1745	C=O (stretch and strong)
	2500 - 3300	O–H (stretch and strong; usually broad)
Ester	1163 – 1210	C–O (stretch strong)
	1715 – 1730	C=O (stretch strong)
	1735 – 1750	C–O (stretch strong)
Ether	1020 – 1075	C–O (stretch strong)
Amine	1020 – 1250	C–N (stretch and medium)
	1080 – 1360	C–N (stretch and medium–weak)
	1600	N–H (bending and medium)
	3300 – 3500	N–H (stretch; medium and 2-bands for primary amine; very weak and 1-band for secondary amine)
Amide	1680 – 1690	C=O (stretch and strong)
Aldehyde	1720 – 1740	C=O (stretch and strong)

RESULTS AND DISCUSSION

Trend Analysis on Effects of Contact Time

The impact of adsorption of both Ni²⁺ and Cr³⁺ on the adsorbent (water hyacinth) was observed to increase with contact time as could be seen in Figure 2. This is in accordance with a past related research [12]. However, Ni²⁺ were adsorbed faster and higher than Cr³⁺ since 92.8% of Ni²⁺ were adsorbed at equilibrium time of 40 minutes compared to 85.7% of Cr³⁺ which were adsorbed at equilibrium time of 50 minutes.

The rapid adsorption of both metal ions at the initial stage could be attributed to the availability of large surface area in the adsorbent. Nevertheless, as the adsorption progressed with time, there was exhaustion of adsorption sites in the adsorbents. Hence, migration of

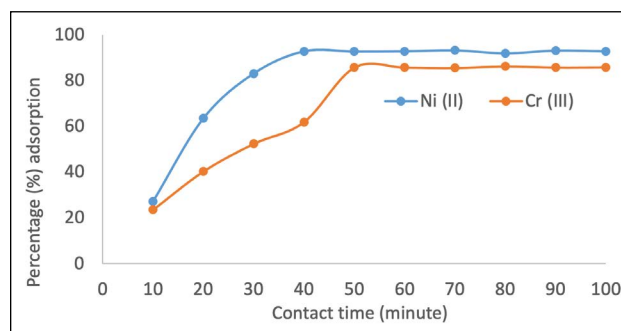


Figure 2. Impact of contact time on adsorption of Ni²⁺ and Cr³⁺ by water hyacinth.

adsorbates from the exterior to the interior sites of the adsorbents took control of the process, which consequently slowed the adsorption rate.

Trend Analysis on Effects of Adsorbent Dosage

Just like the case of contact time, the adsorption of the metal ions (Ni^{2+} and Cr^{3+}) on the water hyacinth adsorbents increased with the dose of the adsorbent applied as could be seen in Figure 3. This observation was also noted in similar researches [12, 13].

Increasing the adsorbent dosage from 0.2g to 1.0g improved the adsorption of Ni^{2+} from 20.6% to 96.3% while that of Cr^{3+} improved from 17.9% to 88.5%. This could be as a result of the fact that more surface areas were available for the adsorption due to accumulation of carbon at higher doses.

Trend Analysis on Effects Initial Adsorbate Concentration

Initial concentration of both adsorbates (Ni^{2+} and Cr^{3+}) showed an inverse relationship with the percentage of their adsorption on the water hyacinth adsorbent, as could be seen in Figure 4. In other words, the adsorption of Ni^{2+} and Cr^{3+} on the adsorbent decreases as their initial concentrations increase, which is in line with a previous related research [14].

Increasing the concentrations of the adsorbates from 1 mg/l to 5 mg/l reduced the adsorption efficiency of Ni^{2+} and Cr^{3+} from 92.6% to 54.0% and 86.3% to 48.4% respectively. This is because the adsorption process occurred by means of the existing sites in the adsorbent binding the metal ions in the adsorbate. Hence, at low concentrations of adsorbates, the readily available sites conveniently binds the metal ions. Since the adsorbent dosages (available sites) were kept constant, the increase in the concentration of adsorbates led to the reduction or saturation of the available binding sites thus, leaving many metal ions not adsorbed thereby reducing the adsorption percentage at higher concentrations.

Trend Analysis on Effect of Solution pH

The effect of solution (adsorbate) pH was observed to be directly proportional to the adsorption efficiency for both metal ions (Ni^{2+} and Cr^{3+}) as the adsorption percentage increased with pH (Fig. 5) thus, affirming an earlier report [15]. This is because at low or acidic pH levels, heavy metals tend to form free cationic species due to the high concentration of hydrogen ions (H^+) associated with low pH. These free cations (H^+) might have been adsorbed on the available binding sites in the adsorbent. In other words at low pH, there is tendency for the adsorbent to be positively charged which definitely repels the metal ions (Ni^{2+} and Cr^{3+}) in the adsorbate and consequently reduced the percentage of adsorption. However as the pH level increased, the reverse process occurred thereby improving the percentage of adsorption.

Despite the explanation given for the improvement of adsorption with increase in pH, the fact remains that the percentage adsorptions for both metal ions at pH 8 and 9 were remarkably high compared to pH 5, 6 and 7 as could be seen in the curves shown in Figure 5. That is, at pH 5,

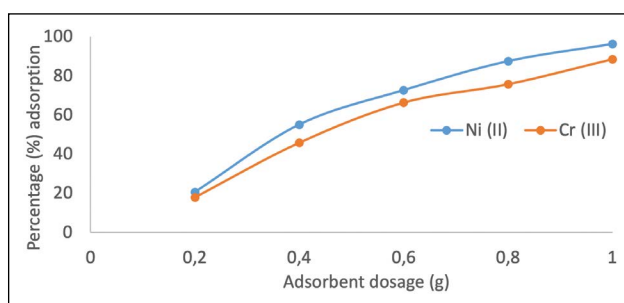


Figure 3. Impact of adsorbent dosage on adsorption of Ni^{2+} and Cr^{3+} by water hyacinth.

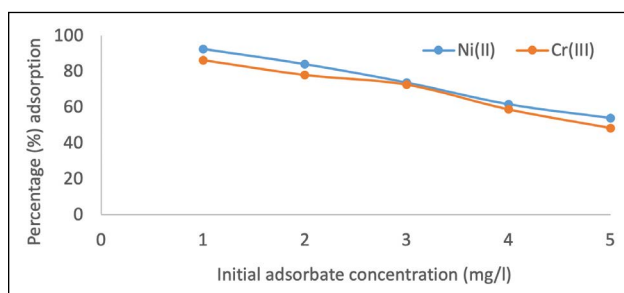


Figure 4. Impact of adsorbate concentration on adsorption of Ni^{2+} and Cr^{3+} by water hyacinth.

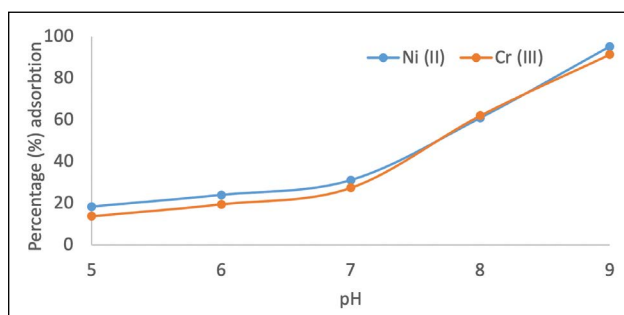


Figure 5. Impact of solution pH on adsorption of Ni^{2+} and Cr^{3+} by water hyacinth.

6, 7, 8, 9, the percentage adsorptions of Ni^{2+} and Cr^{3+} were 18.3, 23.9, 31.0, 60.9, 95.2 and 13.8, 19.5, 27.4, 62.0, 91.3 respectively. These sequences of percentage adsorption for both metal ions clearly revealed that the adsorptions at pH 8 and 9 were very high compared to the lower pH values. This could be attributed to the fact that at pH 8 and 9, the solutions were alkaline thus containing more of hydroxide ions (OH^-) which infused into the binding sites, impart a negative charge on the adsorbent and consequently increased the attractive force between the adsorbent and the metal ions.

Determination of Adsorption Isotherm Parameters

Freundlich Isotherm Model

The parameters for Freundlich isotherm model for the adsorption of Ni^{2+} were obtained through the information given in Figure 6.

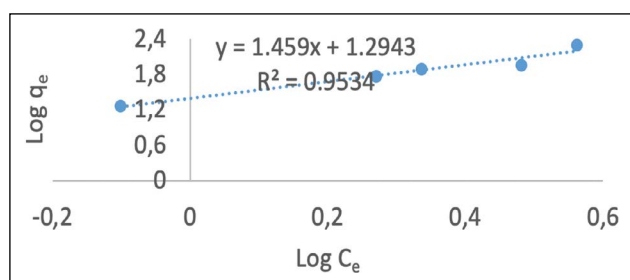


Figure 6. Freundlich isotherm model for adsorption of Ni²⁺ on water hyacinth.

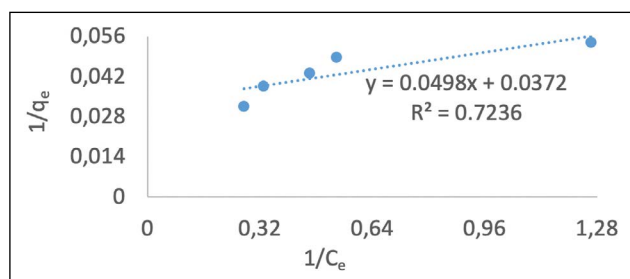


Figure 7. Langmuir isotherm model for adsorption of Ni²⁺ on water hyacinth.

Comparing the Freundlich isotherm model shown in Equation (4) and the equation displayed in Figure 6, implies that the gradient $(\frac{1}{n})=1.459$ hence, $n=0.6854$. Also, the intercept $(\log K_f)=1.2943$ hence, $K_f=10^{1.2943}=19.6925$. In other words, the Freundlich adsorption intensity (n) and capacity (K_f) of the adsorbent (water hyacinth) for the adsorption of Ni²⁺ are 0.6854 and 19.6925 l/g respectively.

Langmuir Isotherm Model

The Langmuir isotherm model for the adsorption of Ni²⁺ is shown in Figure 7 and by comparing it with Equation (5), the parameters were obtained as follows;

The intercept $(\frac{1}{q_m})=0.0372$, hence $q_m=\frac{1}{0.0372}=26.882$. On the other hand, the gradient $(\frac{1}{K_L q_m})=0.0498$ thus, $K_L=\frac{1}{q_m(0.0498)}=\frac{1}{26.882(0.0498)}=0.7470$. This simply implies that the Langmuir monolayer adsorption capacity at equilibrium (q_m) of the adsorbent (water hyacinth) for the adsorption of Ni²⁺ is 26.882 mg/g while the Langmuir equilibrium constant (K_L) is 0.7470l/mg.

Temkin Isotherm Model

The Temkin adsorption constants were determined by comparing Equation (6) and the isotherm model shown in Figure 8. That is, the gradient (β)=96.906 while the intercept ($\beta \ln K_T$)=10.059 hence, $K_T=e^{(10.059/\beta)}=e^{(10.059/96.906)}=e^{0.1038}=1.1094$. Therefore, the heat of sorption (β) and isotherm equilibrium binding (K_T) of the adsorbent (water hyacinth) for the adsorption of Ni²⁺ are 96.906 KJ/mol and 1.1094 l/mg respectively.

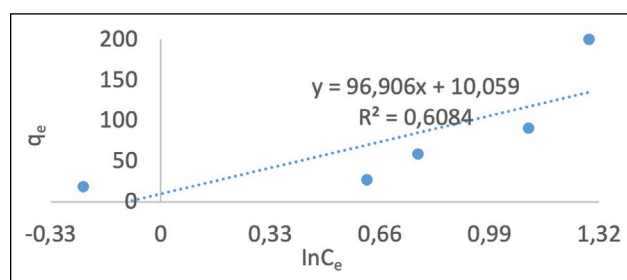


Figure 8. Temkin isotherm model for adsorption of Ni²⁺ on water hyacinth.

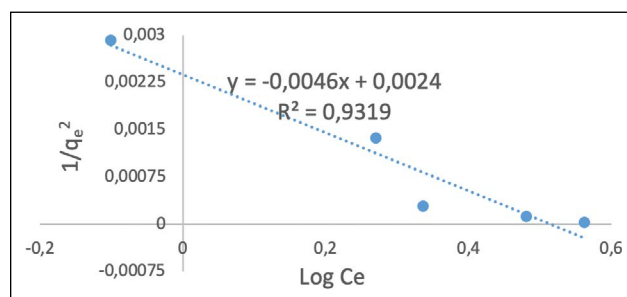


Figure 9. Harkin-Jura isotherm model for adsorption of Ni²⁺ on water hyacinth.

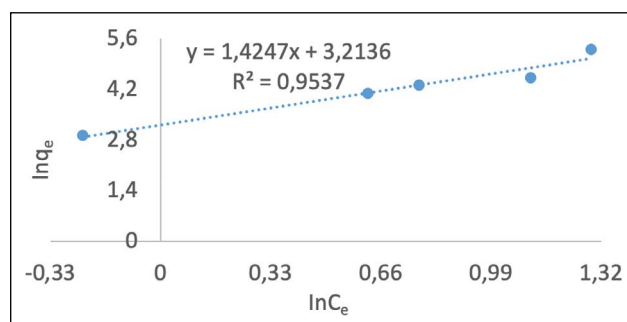


Figure 10. Halsey isotherm models for adsorption of Ni²⁺ on water hyacinth.

Harkin-Jura Isotherm Model

The Harkin-Jura dimensionless constants were obtained by equating the gradient and intercept of Equation (7) to their corresponding values of the model shown in Figure 9 as follows;

Gradient $(-\frac{1}{A})=-0.0046$, hence $A=\frac{1}{0.046}=217.39$.

Similarly, the intercept $(\frac{B}{A})=0.0024$ hence $B=0.0024A=0.0024(217.39)=0.5217$. Consequently, the Harkin-Jura constants A and B of the adsorbent (water hyacinth) for the adsorption of Ni²⁺ are 217.39 and 0.5217 respectively.

Halsey Isotherm Model

Equating the standard linearized form of Halsey isotherm model given in Equation (8) to the linear equation shown in Figure 10, resulted in achieving the Halsey isotherm constants for the adsorbent on the adsorption of Ni²⁺. This is illustrated as follows;

Table 2. Isotherm parameters for adsorption of Ni²⁺ and Cr³⁺ on water hyacinth

Model and parameters	Ni ²⁺	Cr ³⁺
Freundlich model ($\log q_e = \frac{1}{n} \log C_e + \log K_f$)		
<i>n</i>	0.6854	0.5228
<i>K_f</i> (l/g)	19.6925	16.814
R ²	0.9534	0.9488
Langmuir model ($\frac{1}{q_e} = \left(\frac{1}{K_L q_m}\right) \frac{1}{C_e} + \frac{1}{q_m}$)		
<i>q_m</i> (mg/g)	26.882	21.4606
<i>K_L</i> (l/mg)	0.7470	0.7011
R ²	0.7236	0.8353
Temkin model ($q_e = \beta \ln C_e + \beta \ln K_T$)		
β (KJ/mol)	96.906	98.749
<i>K_T</i> (l/mg)	1.1093	0.9623
R ²	0.6084	0.7315
Harkin-Jura model ($\frac{1}{q_e^2} = -\frac{1}{A} \log C_e + \frac{B}{A}$)		
<i>A</i>	217.39	205.08
<i>B</i>	0.5217	0.5104
R ²	0.9319	0.9402
Halsey model ($\ln q_e = -\frac{1}{n} \ln C_e + \frac{1}{n} \ln K_H$)		
<i>n</i>	-0.7019	-0.9347
<i>K_H</i>	0.1048	0.1011
R ²	0.9537	0.9482

Gradient or slope ($-\frac{1}{n}$) = 1.4247, hence $n = \frac{-1}{1.4247} = -0.7019$. On the other hand, the intercept ($\frac{1}{n} \ln K_H$) = 3.2136. It implies $K_H = e^{3.2136n} = e^{3.2136(-0.7019)} = e^{-2.2556} = 0.1048$. Therefore, the Halsey dimensionless constants *n* and *K_H* for the adsorbent (water hyacinth) on the adsorption of Ni²⁺ are -0.7019 and 0.1048 respectively.

The isotherm parameters for the adsorption of Cr³⁺ with respect to Freundlich, Langmuir, Temkin, Harkin-Jura and Halsey models were determined in a similar way as illustrated above, and their obtained values are given in Table 2 alongside with those of Ni²⁺.

The information in Table 2 revealed that R² values greater than 0.9 in both Ni²⁺ and Cr³⁺ adsorptions were recorded in Freundlich, Harkin-Jura and Halsey models, which are all multilayer isotherm models. Hence, the adsorption of Ni²⁺ and Cr³⁺ on the adsorbent (water hyacinth) occurred on heterogeneous surfaces not homogeneous monolayer. Table 2 also informed that the adsorbent (water hyacinth) has higher adsorption capacities on Ni²⁺ than Cr³⁺ while the heat of sorption is higher on Cr³⁺ than Ni²⁺.

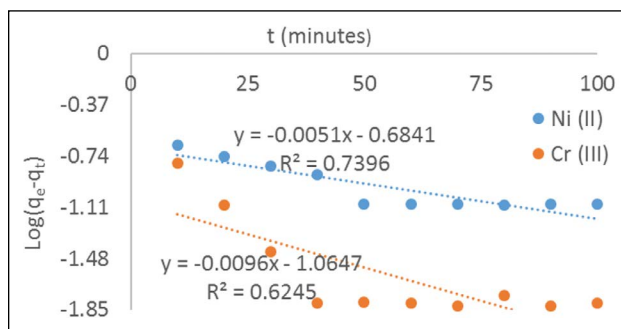


Figure 11. Pseudo 1st-order kinetics for Ni²⁺ and Cr³⁺ adsorption on water hyacinth.

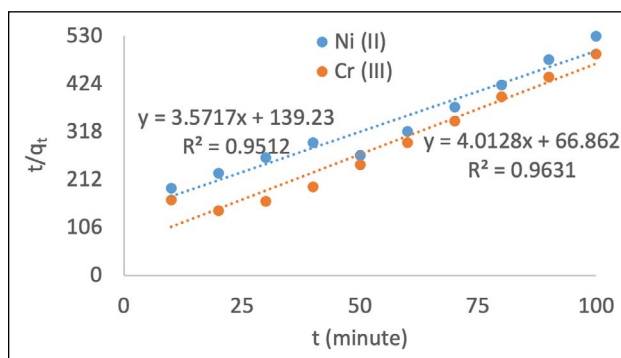


Figure 12. Pseudo 2nd-order kinetics for Ni²⁺ and Cr³⁺ adsorption on water hyacinth.

Table 3. Constants for Pseudo 1st and 2nd order kinetics

Adsorption kinetic and constants	Ni ²⁺	Cr ³⁺
Pseudo 1st - order ($\log(q_e - q_t) = -\left(\frac{k_1}{2.303}\right) t + \log q_e$)		
<i>k₁</i> (min ⁻¹)	0.0117	0.0022
<i>q_e</i> (mg/g)	0.2070	0.0862
R ²	0.7396	0.6245
Pseudo 2nd - order ($\frac{t}{q_t} = \left(\frac{1}{q_e}\right) t + \frac{1}{k_2 q_e^2}$)		
<i>k₂</i> (g.mg ⁻¹ .min ⁻¹)	0.0917	0.2408
<i>q_e</i> (mg/g)	0.2799	0.2492
R ²	0.9512	0.9631

Determination of Adsorption Kinetics Constants

The plots for Pseudo 1st and 2nd order kinetics for the adsorption of both ions are shown in Figure 11 and 12 respectively. The constants for Pseudo 1st-order kinetic for both ions were obtained by comparing Equation (10) and the equations displayed in Figure 11. Similarly, Equation (11) was compared with the equations shown in Figure 12 to obtain the constants for Pseudo 2nd-order kinetic for both ions. The determined values are presented in Table 3.

The information shown in Table 3 revealed that the R² values for both Ni²⁺ and Cr³⁺ in Pseudo 2nd order kinetics were higher than 0.95 unlike those of Pseudo 1st-order kinetic that were less than 0.75 for both ions. This implies that the

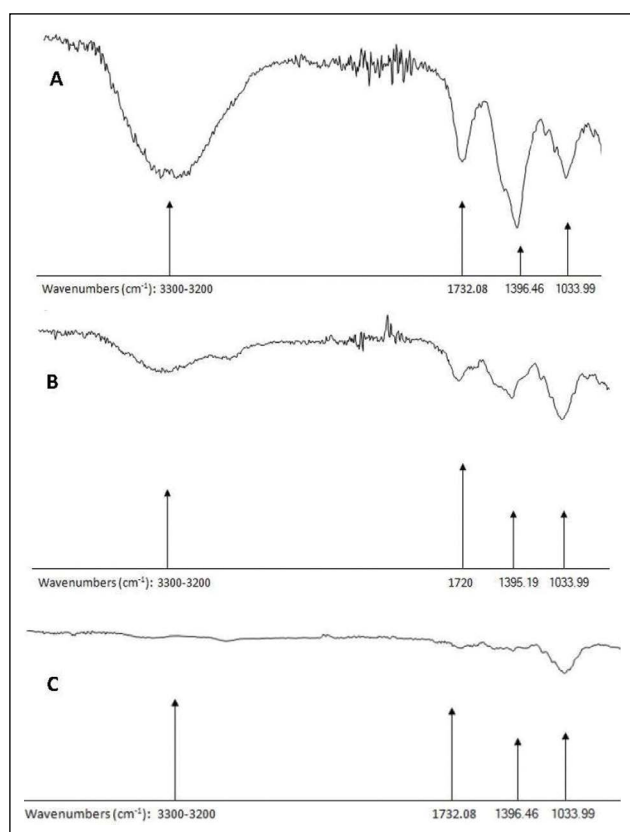


Figure 13. FT-IR spectra of water hyacinth before adsorption, after adsorption of Ni^{2+} and after adsorption of Cr^{3+} .

pathway or mechanism of the adsorption process for both ions (Ni^{2+} and Cr^{3+}) followed Pseudo 2nd-order kinetics. This assertion is in line with related researches [9, 16]. Table 3 also inform that the equilibrium adsorptions (q_e) for both Pseudo 1st and 2nd order kinetics were higher in the adsorption of Ni^{2+} than Cr^{3+} however, Ni^{2+} has higher rate constant in Pseudo 1st order kinetics and lower rate constant in Pseudo 2nd order kinetics compared to Cr^{3+} .

Trend Analysis of FT-IR

The FT-IR spectroscopy of the adsorbent before and after adsorption of the ions (Ni^{2+} and Cr^{3+}) revealed that the functional groups present in both cases varies within the scanning range of 4000 cm^{-1} to 400 cm^{-1} as could be seen in Figure 13. Prior to adsorption, a broad absorption band within 3300 to 3200 cm^{-1} was observed in the adsorbent (water hyacinth) with a strong intensity (Fig. 13a). This is an attribute of stretches of O-H emanating from alcohol and carboxylic acid. However, the absorption band (3300 to 3200 cm^{-1}) reduced in intensity after the adsorption of Ni^{2+} (Fig. 13b) but disappeared after the adsorption of Cr^{3+} (Fig. 13c).

Other absorption peaks observed in the adsorbent (water hyacinth) prior to the adsorption process were at wavenumbers 1732.08 cm^{-1} , 1396.46 cm^{-1} and 1033.99 cm^{-1} . Wave number 1732.08 cm^{-1} indicates stretches of C=O from car-

boxylic acid and aldehyde, 1396.46 cm^{-1} is a feature of bending vibrations of C-H from alkane as well as O-H from alcohol and carboxylic acid while 1033.99 cm^{-1} is a characteristics of stretches of C-O from alcohol and ether as well as stretches of C-N from amine. However, after the adsorption of Ni^{2+} (Fig. 13b), wavenumbers 1732.08 cm^{-1} and 1396.46 cm^{-1} shifted to 1720 cm^{-1} and 1395.19 cm^{-1} respectively with reduced intensities, but disappeared after the adsorption of Cr^{3+} (Fig. 13c). Wave numbers 1732.08 cm^{-1} indicate stretches of C=O from carboxylic acid and aldehyde while 1720 cm^{-1} suggests stretches of C=O from ester and aldehyde. Also, wavenumbers 1396.46 cm^{-1} and 1395.19 cm^{-1} are features of bending vibrations of C-H from alkane as well as O-H from alcohol and carboxylic acid while 1033.99 cm^{-1} is a characteristics of stretches of C-O from alcohol and ether as well as stretches of C-N from amine.

The disappearance of the absorption peaks 3300 to 3200 cm^{-1} , 173.08 cm^{-1} and 1396.46 cm^{-1} after the adsorption of Cr^{3+} might be due to the binding of Cr^{3+} on the hydroxyl (O-H) and carbonyl (C=O) groups present in the adsorbent. In general, the shift in absorption peaks and reduction in intensity suggest that the corresponding functional groups were responsible for the ion adsorptions in the binding sites. The presence of these functional groups were also noted in a similar research [17].

CONCLUSIONS AND RECOMMENDATIONS

From the analysed data carried out in this research, it could be concluded that water hyacinth could be used effectively in adsorbing Ni^{2+} and Cr^{3+} in wastewater as their adsorption capacities were quite high however, the adsorption capacities were higher in Ni^{2+} than Cr^{3+} while the heat of sorption is higher in Cr^{3+} than Ni^{2+} . The adsorption of Ni^{2+} and Cr^{3+} on water hyacinth occurred on heterogeneous surfaces (not homogenous monolayers) as their data points fitted well in multilayer models such as Freundlich, Harking-Jura and Halsey models. In addition, the pathway or mechanism of the adsorption process for both Ni^{2+} and Cr^{3+} followed Pseudo 2nd-order kinetics. Furthermore, the functional groups involved in the binding sites were alkane, alcohol, carboxylic acid, ester, ether, amine and aldehyde however, hydroxyl group (O-H) from alcohol and carboxylic acid participated more. It is recommended that water hyacinth should be used as a potential bio-adsorbent to remove heavy metals especially Nickel and Chromium from wastewater since its adsorption capacity is quite high and its availability is abundant.

DATA AVAILABILITY STATEMENT

The authors confirm that the data that supports the findings of this study are available within the article. Raw data that support the finding of this study are available from the corresponding author, upon reasonable request.

CONFLICT OF INTEREST

The authors declared no potential conflicts of interest with respect to the research, authorship, and/or publication of this article.

ETHICS

There are no ethical issues with the publication of this manuscript.

REFERENCES

- [1] P.N. Obasi and B.B. Akudinobi, "Potential health risk and levels of heavy metals in water resources of lead–zinc mining communities of Abakaliki, South-east Nigeria", *Applied Water Science*, Vol. 10, pp. 2-23, 2020.
- [2] G.K. Kinuthia, V. Ngure, D. Beti, R. Lugalia, A. Wangila and L. Kamau, "Levels of heavy metals in wastewater and soil samples from open drainage channels in Nairobi, Kenya: Community health implication", *Scientific Reports*, Article 8434.
- [3] D.B. Bahiru, "Determination of heavy metals in wastewater and their toxicological implications around eastern industrial zone, Central Ethiopia", *Journal of Environmental Chemistry and Ecotoxicology*. Vol. 12, pp. 72-79, 2019.
- [4] A. Kharazi, M. Leli and M. Khazali, "Human health risk assessment of heavy metals in agricultural soil and food crops in Hamadan, Iran," *Journal of Food Consumption Analysis*, Vol. 100, pp. 1-16, 2021.
- [5] L.G. Gomah, R.S. Ngumbu and R.B. Voegborlo, "Dietary exposure to heavy metal contaminated rice and health risk to the population of Monrovia," *Journal of Environmental Science and Public Health*, Vol. 3, pp. 474-482, 2019.
- [6] J. Pal, M. Bishnoi and M. Kaur, "Heavy metals in soil and vegetables and their effect on health," *International Journal of Engineering Science Technologies*, Vol. 2, pp. 17-27, 2017.
- [7] S. Tabrez, T.A. Zughaibi and M. Javed, "Bioaccumulation of heavy metals and their toxicity assessment in mystus species," *Saudi Journal of Biological Sciences*, Vol. 28, pp. 1459-1466, 2021.
- [8] F.J. Ogbozige and M.A. Toko, "Adsorption isotherms and kinetics of lead and cadmium ions: Comparative studies using modified melon (*Citrullus colocynthis*) husk," *Iranian (Iranica) Journal of Energy & Environment*, Vol. 11, pp. 157-162, 2020.
- [9] A. Yirga, Y. Werede, G. Nigussie and F. Ibrahim, "Dried orange peel: A potential biosorbent for removal of Cu (ii) and Cd (ii) ions from aqueous solution," *To Chemistry Journal*, Vol. 7, pp. 124-141, 2020.
- [10] J.M. Mahlangu, G.S. Simate and M. de Beer, "Adsorption of Mn²⁺ from the acid mine drainage using banana peel," *International Journal of Water and Wastewater Treatment*, Vol. 4, pp. 153-159, 2018.
- [11] H. Ali, E. Khan and I. Ilahi, "Environmental chemistry and ecotoxicology of hazardous heavy metals: Environmental persistence, toxicity, and bioaccumulation," *Journal of Chemistry*, pp. 1-14, 2019.
- [12] B.I. Okolo, E.O. Oke, C.M. Agul, O. Adeyi, K. Nwoso-Obieogu and K.N. Akatobi, "Adsorption of lead(II) from aqueous solution using Africa elemi seed, mucuna shell and oyster shell as adsorbents and optimization using Box–Behnken design," *Applied Water Science*, Vol. 10, pp. 1-23, 2020.
- [13] O.J. Akinyeye, T.B. Ibigbami, O.O. Odeja and O.M. Sosanolu, "Evaluation of kinetics and equilibrium studies of biosorption potentials of bamboo stem biomass for removal of lead (II) and cadmium (II) ions from aqueous solution," *African Journal of Pure and Applied Chemistry*, Vol. 14, pp. 24-41, 2020.
- [14] E. Solgi and A. Zamanian, "Biosorption of chromium and nickel from aqueous solution by chicken feather," *Archives of Hygiene Sciences*, Vol. 9, pp. 97-108, 2020.
- [15] S.Gupta and A. Kumar, "Removal of Nickel (II) from Aqueous Solution by Biosorption on *A. barbadensis* Miller Waste leaves Powder," *Applied Water Science*, Vol. 9, pp. 1-11, 2019.
- [16] T.S. Badessa, E. Wakuma and A.M. Yimer, "Biosorption for effective removal of chromium(VI) from wastewater using *Moringa stenopetala* seed powder (MSSP) and banana peel powder (BPP)," *BMC Chemistry*, Vol. 14, pp. 1-12, 2020.
- [17] P.W. Ndung'u, G. Mwithiga, C.N. Onyari, G. Muriithi and S.T. Mukono, "Evaluating the surface functional groups on banana leaf petioles and the resultant biochar for potential adsorbance," *Journal of Materials and Environmental Sciences*, Vol. 11, pp. 255-261, 2020.